

Development of a Road/Terrain Characterization Rating Tool

J. Gavin Howe, Dongchan Lee, Chi Liang, Jeffrey P. Chrstos,
Thomas T. Myers, R. Wade Allen
Systems Technology, Inc.

David J. Gorsich, Andrew J. Scott
U.S. Army Tank-automotive and Armaments Command

Copyright © 2003 SAE International

ABSTRACT

The U.S. Army currently uses the root mean square of elevation and power spectral density to characterize road/terrain (off-road) roughness for durability. This paper describes research aimed toward improving these metrics. One method currently under consideration involves running a relatively simple, yet vehicle class specific, model over a given terrain and using predicted vehicle response(s) to classify or characterize the terrain. A precedent for this concept is the International Roughness Index or IRI, used in the highway industry to rate road roughness. This paper will provide a summary of the research done to date on this problem.

INTRODUCTION

Properly characterizing terrain roughness is an important issue for the U.S. Army. Currently, in the procurement of new vehicles, the Army specifies the roughness of the test course to which the vehicle would be subjected during testing. This specification comes in the form of a root mean square elevation (RMSE) or a power spectral density (PSD). The Army uses RMSE to characterize roughness of the terrain because it is a simple single measure. As an example, cross-country terrain driving is classified as having a 0.8 to 1.8 inch RMSE [1].

The RMSE is a single number that represents the roughness of the courses or the roughness of the terrain where actual vehicles are being tested. The simulations that use RMSE as a test for roughness cannot be validated or correlated to experiment. The dangers of misclassification of terrain roughness include vehicle malfunctions, subsequent required equipment modifications, excessive maintenance efforts, and revisions and restarts of the test program [2].

Using RMSE requires that some strong statistical assumptions hold for the test course. The course is assumed to be stationary, Gaussian, and to be a one-dimensional time series. While some of these assumptions may be true for a particular course and/or

terrain, more often than not, one or more of the above assumptions is not true.

This paper describes an alternative approach to characterizing test courses. This approach involves examining the response(s) of a simple vehicle model driven over the terrain/test course and developing a rating scheme to characterize the roughness of the terrain. One example of this type of rating that is already being used in the highway community to measure roadway roughness is the International Roughness Index (IRI). This paper presents very preliminary results of further extensions and refinements related to appropriate tire models and incorporation of fatigue analysis concepts into the terrain rating process. The research for this effort is in the early stages, but an overview of the approach and some preliminary results are presented in this paper.

APPROACH

The goal of this research is to develop a system for rating terrain and/or test courses based on the response(s) of a relatively simple vehicle model driven over the terrain profile. Several questions need to be answered to achieve this goal. They include the following:

- What level of sophistication is required for the vehicle model?
- What level of sophistication is required for the tire model used in conjunction with the vehicle model?
- What should the parameters be for the given model?
- What vehicle response(s) should be considered when developing a metric or rating scheme?
- What vehicle model speed(s) should be used when rating the terrain?
- How should the wide range of vehicle classes and types be treated?
- How can the terrain rating be related to the mechanics of fatigue failure?

Report Documentation Page			Form Approved OMB No. 0704-0188		
Public reporting burden for the collection of information is estimated to average 1 hour per response, including the time for reviewing instructions, searching existing data sources, gathering and maintaining the data needed, and completing and reviewing the collection of information. Send comments regarding this burden estimate or any other aspect of this collection of information, including suggestions for reducing this burden, to Washington Headquarters Services, Directorate for Information Operations and Reports, 1215 Jefferson Davis Highway, Suite 1204, Arlington VA 22202-4302. Respondents should be aware that notwithstanding any other provision of law, no person shall be subject to a penalty for failing to comply with a collection of information if it does not display a currently valid OMB control number.					
1. REPORT DATE 04 AUG 2003		2. REPORT TYPE Journal Article		3. DATES COVERED 05-07-2003 to 03-08-2003	
4. TITLE AND SUBTITLE Development of a Road/Terrain Characterization Rating Total		5a. CONTRACT NUMBER			
		5b. GRANT NUMBER			
		5c. PROGRAM ELEMENT NUMBER			
6. AUTHOR(S) J. Gavin Howe; Dongchan Lee; Chi Liang; Jeffrey Chrstos; Thomas Myers		5d. PROJECT NUMBER			
		5e. TASK NUMBER			
		5f. WORK UNIT NUMBER			
7. PERFORMING ORGANIZATION NAME(S) AND ADDRESS(ES) Systems Technology, Inc.,13766 Hawthorne Boulevard,Hawthorne,CA,90250		8. PERFORMING ORGANIZATION REPORT NUMBER ; #13928			
9. SPONSORING/MONITORING AGENCY NAME(S) AND ADDRESS(ES) U.S. Army TARDEC, 6501 East Eleven Mile Rd, Warren, Mi, 48397-5000		10. SPONSOR/MONITOR'S ACRONYM(S) TARDEC			
		11. SPONSOR/MONITOR'S REPORT NUMBER(S) #13928			
12. DISTRIBUTION/AVAILABILITY STATEMENT Approved for public release; distribution unlimited					
13. SUPPLEMENTARY NOTES Submitted to 2003 SAE International					
14. ABSTRACT The U.S. Anny currently uses the root mean square of elevation and power spectral density to characterize road/terrain (off-road) roughness for durability. This paper describes research aimed toward improving these metrics. One method currently under consideration involves running a relatively simple, yet vehicle class specific, model over a given terrain and using predicted vehicle response(s) to classify or characterize the terrain. A precedent for this concept is the International Roughness Index or IRI, used in the highway industry to rate road roughness. This paper will provide a summary of the research done to date on this problem.					
15. SUBJECT TERMS					
16. SECURITY CLASSIFICATION OF:			17. LIMITATION OF ABSTRACT Public Release	18. NUMBER OF PAGES 11	19a. NAME OF RESPONSIBLE PERSON
a. REPORT unclassified	b. ABSTRACT unclassified	c. THIS PAGE unclassified			

When determining the level of sophistication required for the vehicle and tire models, the general approach will be to start with very simple models and to increase the complexity until little further increase in predicting the true nature of the terrain roughness is gained.

If we have two distinct vehicle models for rating the terrain, one simplified with respect to the other, will they produce similar or distinct terrain rating(s)?

The terrain rating modeling criterion is:

If the simpler model produces essentially the same rating as the higher order model, then the former is an adequate approximation; otherwise it is not.

The parameters for the vehicle and tire models will likely be based on the class of vehicle being procured.

Since the terrain rating will be used to generate or specify terrain for assessment of vehicle durability, it is thought that the rating procedure should be formally related to durability. Of all the factors that influence vehicle durability, fatigue failure of components is most significantly related to terrain characteristics. Thus, fatigue prediction based on stresses developed in an arbitrary part subjected to force(s) in the vehicle model caused by driving over the terrain is being investigated as a basis for directly relating terrain characteristics to durability.

A range of speeds will be evaluated depending on the roughness of the terrain and the class of vehicle being assessed.

An example of a relatively simple vehicle model being used to rate roadways is the IRI. A brief overview of the IRI is presented below.

OVERVIEW OF THE IRI

The IRI was developed over several decades. The following bullets are taken from a summary of the IRI evolution found in [1].

- Routine analysis of road profiles began shortly after the GM profiler was developed in the late 1960's.
- One of the first research applications combined measured profiles with a quarter car model that replicated the Bureau of Public Roads (BPR) Roughometer – a one-wheeled trailer with a road meter.
- In the late 1970's, National Cooperative Highway Research Program (NCHRP) sponsored a study of response-type road roughness measuring systems like the BPR Roughometer.
- An objective of this study was to develop calibration methods for the response-type systems – the researchers concluded that the only valid method was to calibrate by correlation against a defined roughness index.

- The best correlation was obtained with a set of parameters called the "Golden Car."
- The Golden Car spring rate parameters were chosen to match the two major resonant frequencies (body and axle bounce) for a circa 1978 vehicle, but the damping is much higher than most cars and trucks. This was done to improve correlation with a wide variety of response-type systems.
- The Golden Car was one of the candidate references considered for the IRI and was selected.
- A speed of 80 km/hr was chosen as the standard speed for the simulation.

The IRI is computed from a single longitudinal profile. The sample interval for the profile should be no larger than 300 mm for accurate calculations. The required resolution depends on the roughness level with finer resolution being needed for smooth roads. The profile is assumed to have constant slope between sampled elevation points. The profile is smoothed with a moving average whose base length is 250 mm. The smoothed profile is filtered using a quarter-car simulation (Golden Car) with a simulated speed of 80 km/hr. The simulated suspension motion is linearly accumulated and divided by the length of the profile to get IRI (IRI has units of slope).

IRI ALGORITHMS AND CALCULATIONS

The IRI contains two filters: a moving average filter on the terrain height (tire model), and a quarter car model. The moving average filter, which is a first order approximation of a tire's terrain enveloping behavior, generates a smoothed profile height (h_{ps}) from the original profile (h_p) and is defined as:

$$h_{ps}(i) = \frac{1}{k} \sum_{j=i}^{i+k-1} h_p(j)$$

where

$$k = \max \left[1, \text{round} \left(\frac{L_B}{\Delta} \right) \right] \quad (1)$$

and

L_B = moving average base length, 250 mm
 Δ = sample interval

A sine sweep was created to show the input/output relationship for the moving average filter. The results are given in Figure 1. The transfer function for the moving average filter is given in Figure 2. Three base lengths are shown in this figure: 0.125, 0.25 (IRI base length), and 0.5 m. This figure shows that the moving average filter is essentially a low pass filter and that the longer the base length, the lower the cut-off frequency.

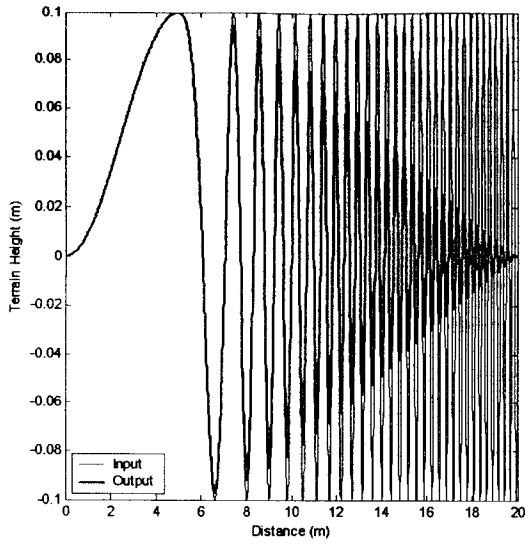


Figure 1 - IRI Tire Model "Time Domain" Response

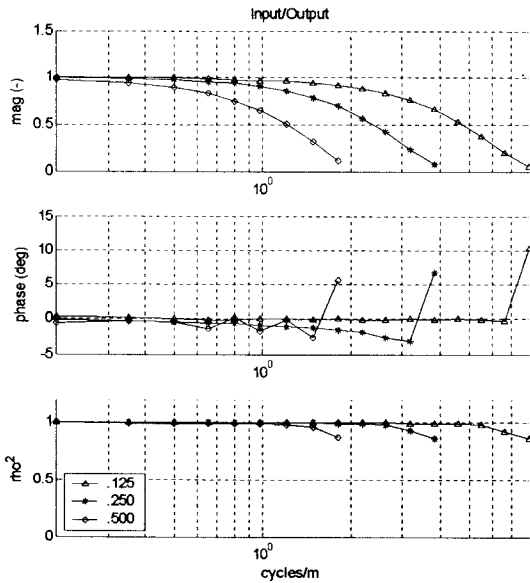


Figure 2 - IRI Tire Enveloping Model Frequency Response

The IRI quarter car model is shown in Figure 3.

The quarter car equations of motion were derived as:

Sprung Mass

$$m_s \ddot{z}_s = k_s (z_u - z_s) + c_s (\dot{z}_u - \dot{z}_s) \quad (2)$$

Unsprung Mass

$$m_u \ddot{z}_u = -k_s (z_u - z_s) - c_s (\dot{z}_u - \dot{z}_s) + k_t (h - z_u)$$

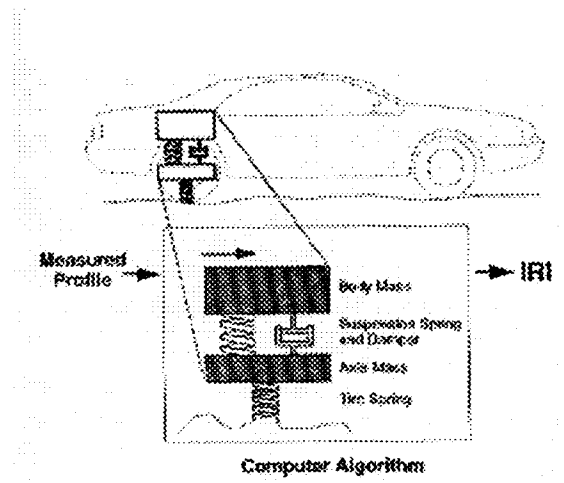


Figure 3 – IRI Quarter Car Model [3]

Where m_s and m_u are the sprung and unsprung masses, k_s and k_t are the spring and tire stiffness, c_s is the damper coefficient, z_s and z_u are the sprung and unsprung mass displacements, and h is the profile height. In the implementation of the IRI, equations given in (2) are normalized for the sprung mass.

Sprung Mass

$$\ddot{z}_s = k_2 (z_u - z_s) + c (\dot{z}_u - \dot{z}_s) \quad (3)$$

Unsprung Mass

$$\mu \ddot{z}_u = -k_2 (z_u - z_s) - c (\dot{z}_u - \dot{z}_s) + k_1 (h - z_u)$$

The IRI Golden Car parameters are:

$$\begin{aligned} c &= c_s / m_s = 6.0 \quad (s^{-1}) \\ k_1 &= k_t / m_s = 653 \quad (s^{-2}) \\ k_2 &= k_s / m_s = 63.3 \quad (s^{-2}) \\ \mu &= m_u / m_s = 0.15 \quad (-) \end{aligned} \quad (4)$$

The IRI is defined as the simulated motion of the sprung and unsprung masses normalized by the length of the profile:

$$IRI = \frac{1}{L} \int_0^{L/V} |\dot{z}_s - \dot{z}_u| dt \quad (5)$$

The IRI gain response is shown in Figure 4. It is essentially a band pass filter. The first and second peaks represent the body heave and wheel bounce vibration modes, respectively.

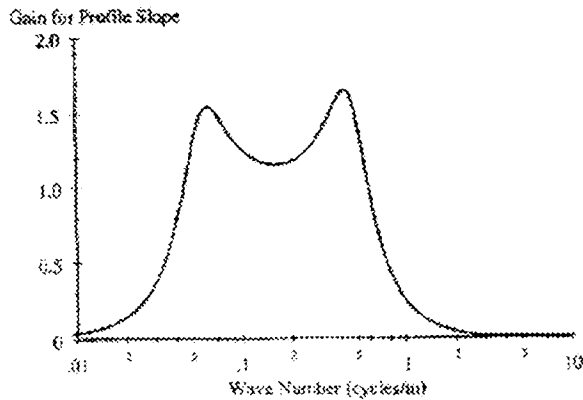


Figure 4 – IRI Filter Gain [4]

Modification of the vehicle model parameters could result in a very different band pass filter frequency range and could change the general shape for the gain response. Higher order models could also result in very different responses.

TIRE MODELING

As discussed previously, the IRI tire-enveloping model is a simple moving average. This model is subject to an “aliasing like” effect at wave numbers above 1/tire contact patch length ($1/0.25 \text{ m} = 4 \text{ cycles/m}$ for the IRI). The “aliasing” is not due to low sampling frequency, but instead due to averaging over more than one cycle, i.e., the tire contact patch is covering more than 1 cycle of input. The sine sweep response given in Figure 1 was extended to higher wave numbers as shown in Figure 5. After reaching zero response at 4 cycles/m, the response starts to increase due to the averaging of more than 1 cycle. The moving average tire model essentially assumes that there is no tread band stiffness, i.e., that the tire tread follows the road profile, even if it means following down into a very narrow “crack”, and that the average height of the tread over the length of the contact patch is the input to the tire spring stiffness. This tire model is suitable for relatively smooth road profiles, but will not be appropriate for rougher off-road terrains.

A literature search for potential tire models has been performed. The observed tire model complexity ranged from a point contact follower up to finite element models. While the point contact follower model is believed to be too simple, the finite element models are far too complex for the purposes of developing a terrain rating. Several model types of intermediate complexity appear to yield reasonable results.

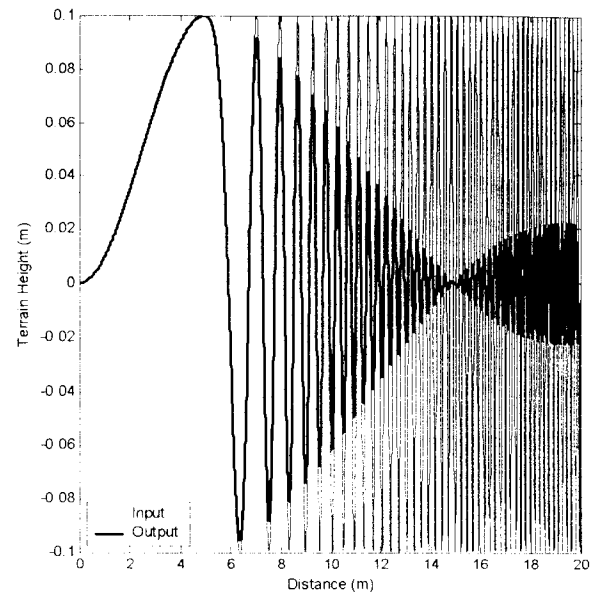


Figure 5 – “Aliasing” with the IRI Moving Average Filter

One such model is a rigid roller or effective road input tire model. The theoretical derivation of this effective road profile is the wheel center trace when the vehicle travels very slowly over the real ground profile (Figure 6). The question is how to find this effective road profile corresponding to the real ground profile. The easiest way to calculate the effective road profile is to assume the tire is a rigid disk [5]. Based on this geometric restriction, the effective road profile can be easily calculated. The rigid roller model essentially filters the high frequency road input to provide a more realistic input for a point contact tire model. However, this model ignores the tire-enveloping characteristic. The calculated effective road profile departs from the measured one; especially at sharp corners contained in the original road profile.

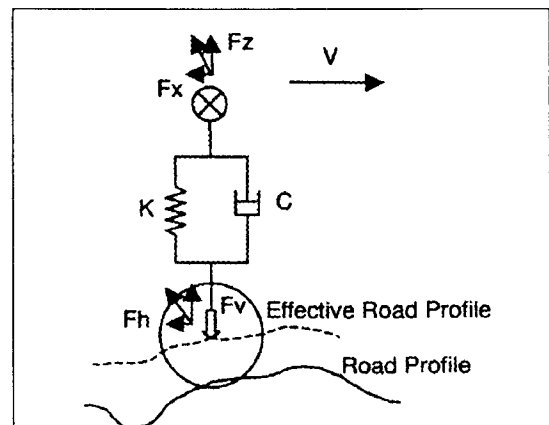


Figure 6 - Effective Road Input [11]

The frequency and time domain responses for the rigid roller tire model are shown in Figure 7 and Figure 8, respectively. Instead of contact patch length, as was the case for the IRI tire model, the different lengths correspond to the radius of the tire. The frequency response is somewhat similar to that for the IRI tire model in that it rolls off at lower frequencies as the tire radius increases. It tends to have a higher magnitude at lower frequencies that increases with decreasing tire radius. The time domain response is very similar to the input at low frequencies. The time domain response seems more realistic for this model than the simple moving average in that it rides the top of the road profile when the wave numbers (cycles/m) are large. The frequency response at the low range should be 1, but there was not high enough power in the input at the low frequency range to produce this. A second sine sweep was run at lower frequencies. The frequency and time domain responses showed that the frequency response magnitude is 1 at low frequency. The initial work performed with this model suggested that the response was too stiff.

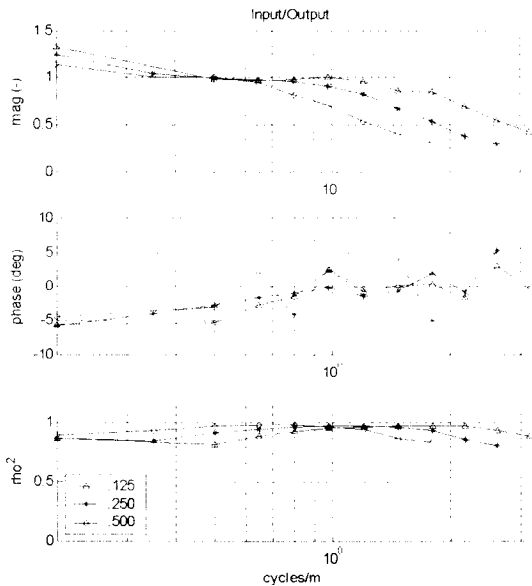


Figure 7 - Rigid Tire Model Frequency Response

The next tire model that will be examined is a flexible roller tire model [6]. The flexible roller contact model includes the contact pressure distribution on the tire contact patch and filters the ground profile within the contact patch. There are several ways to determine the contact pressure distribution. Measurement of the contact pressure distribution would be the most accurate. This distribution could also be calculated by assuming the shape of the distribution. The simplest one is the uniform contact pressure distribution assumption. This model assumes the tire stiffness is distributed uniformly over the contact patch and it approaches the rigid roller contact model as the distributed stiffness approaches infinity. This model does not simulate the tire tread bending effect and

carcass bulging effect. The model and example contact pressure distribution are shown in Figure 9.

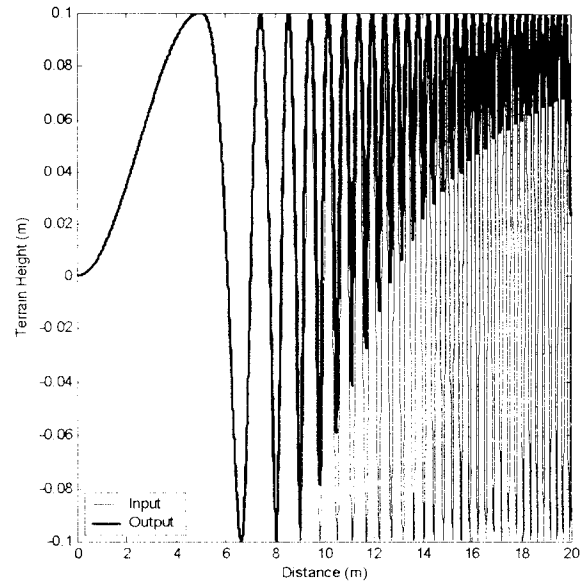


Figure 8 - Rigid Tire Model "Time Domain" Response Overlaid on Input

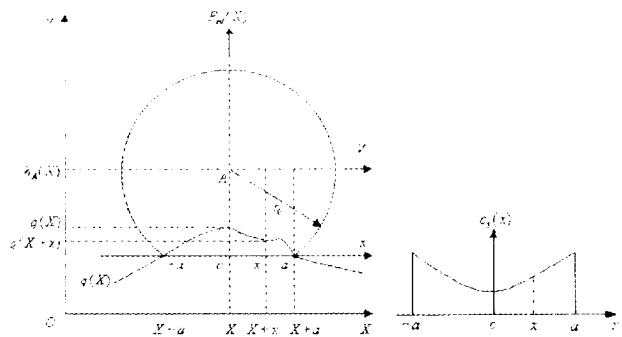


Figure 9 - Flexible Roller Contact Model and Contact Pressure Distribution

VEHICLE MODELING

A range of vehicle models will be examined during this study including quarter car, half-car pitch plane, and full vehicle models. The quarter car has been the focus up to this point.

The quarter car model for the IRI is implemented using a state space solution. While the particular state space solution is very efficient, it is not useful for analyzing the addition of any non-linearity to the model. An Explicit Euler integration method to solve the quarter car model was developed. To achieve better agreement with the state space solutions, additional linearly interpolated

points are added to the profile. It was found that adding 100 linearly interpolated points between each data sample gave similar results for the two solution methods.

One of the goals for using the Explicit Euler integration method was to look at the tire and suspension forces. These forces are not fully modeled in Equation (2) because the initial deflection of the tire and suspension due to the effect of gravity on the sprung and unsprung masses has not been accounted for. Not including this effect generally does not change the calculation of the IRI (unless the wheels come off the ground which generally is not the case for road profiles). Accounting for the initial tire and suspension forces yields:

Sprung Mass

$$m_s \ddot{z}_s = -m_s g + k_s (z_u - z_s) + F_{s,0} + c(\dot{z}_u - \dot{z}_s)$$

Unsprung Mass

$$m_u \ddot{z}_u = -m_u g - k_s (z_u - z_s) - F_{s,0} - c(\dot{z}_u - \dot{z}_s) + k_t (h - z_u) + F_{t,0} \quad (6)$$

Where $F_{s,0}$ and $F_{t,0}$ are the initial suspension spring and tire forces and $k_s (z_u - z_s) + F_{s,0}$ and $k_t (h - z_u) + F_{t,0}$ are the total suspension spring and tire forces. At static equilibrium:

$$\begin{aligned} F_{s,0} &= m_s g \\ F_{t,0} &= (m_u + m_s) g \end{aligned} \quad (7)$$

TERRAIN RATING METRICS

Several terrain rating metrics have been examined. They include IRI, Speed Roughness Index (IRI x Speed), and Repetitions to Failure. The latter metric represents a very preliminary assessment of how the mechanics of fatigue failure, which are not addressed in the IRI, might be introduced into the terrain rating process. During these evaluations, the quarter car model speed was varied from 1 to 80 km/hr, while the IRI metric is run at a single speed, namely 80 km/h. The gain response for the quarter car model with the IRI parameters for multiple speeds is given in Figure 10. The gain response for the quarter car model does change with vehicle speed. The basic shape of the response does not change because the vehicle parameters are not speed dependent and the quarter car model is linear, but it does shift down the wave number spectrum as speed increases.

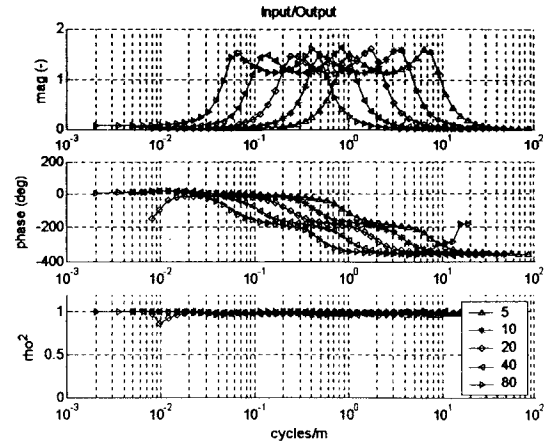


Figure 10 – IRI Quarter Car Gain Response at Multiple Speeds

INTERNATIONAL ROUGHNESS INDEX (IRI)

The IRI quarter car model, in conjunction with the IRI tire model, was run over 500-cycle sinusoidal terrains with wave numbers ranging from 0.01 to 3.7 cycles/meter. The magnitude of the sinusoidal input was 0.001 meters. The vehicle speed ranged from 1 to 80 km/h. The IRI calculated values are given in the Figure 11 contour plot. The values are plotted as a function of speed and wave number. The color bar on the side of the figure indicate dark areas represent low IRI values and light areas represent high IRI values. The units of the IRI values are m/km. The dark areas represent wave numbers that are either above or below the IRI band pass filter for a given speed. The lower the speed, the wider the band pass filter appears. This seems inconsistent with what was shown for the IRI quarter car gain responses in Figure 10. The gain responses in Figure 10 are plotted on a logarithmic scale, while the contour plot is not. A surface (or 3-dimensional) plot for the same data is given in Figure 12.

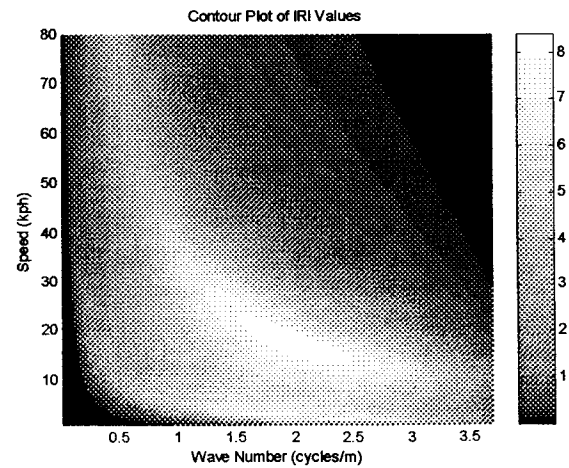


Figure 11 – Contour Plot of IRI Values as a Function of Wave Number and Speed

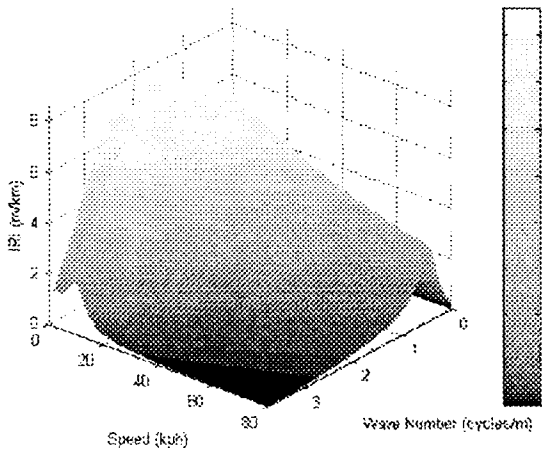


Figure 12 – Surface Plot of IRI Values as a Function of Wave Number and Speed

Initially, it is somewhat surprising that the IRI values for a given wave number increase with a decrease in speed, down to lower speeds where there is some waviness or undulations in the response. To visualize this more clearly, IRI values for a few wave numbers are plotted as a function of speed in Figure 13. These responses look very much like the gain responses for the IRI quarter car model shown in Figure 10. Examining the 1.5 cycle/m trace, the IRI values are very low at 80 km/h and increase down to approximately 23 km/h. This suggests that road roughness decreases with an increase in speed. Below 23 km/h, there is a dip, followed by another peak at approximately 3 km/h and then a decrease down to 1 km/h. The other traces have this same basic trend, with peaks and valleys occurring at different speeds. A line is drawn on this plot at an IRI of 3 m/km. This line passes through the 0.5 cycles/m wave number at 10, 58, and 80 km/h. Is the road roughness at these speeds and wave number the same? To examine this more closely, the vehicle responses at 0.5 cycles/m and 10, 58, and 80 km/h were examined in detail.

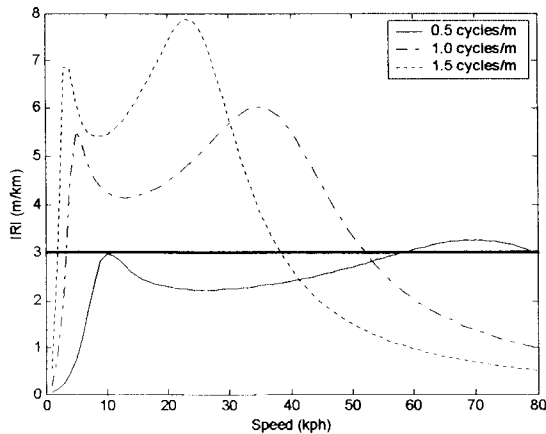


Figure 13 – IRI Values as a Function of Speed for Specific Wave Numbers

The sprung mass displacement, unsprung mass displacement, and profile height for the 0.5 cycle/m wave number at 10, 58, and 80 km/h are plotted in Figure 14. The sprung mass displacements for the 58 and 80 km/h traces are much smaller than those for the 10 km/h trace, while the unsprung mass displacements are slightly larger. The profile is the same for all three traces.

The sprung mass, unsprung mass, sprung mass – unsprung mass, and profile velocities are plotted in Figure 15. While the sprung mass velocity for the 10 kph trace is slightly higher than the 58 and 80 km/h traces, the unsprung mass, sprung – unsprung mass, and profile velocities are much lower for the 10 kph speed. The 58 km/h traces are somewhat lower than the 80 km/h traces. As noted in Equation (5), the IRI calculation is based on the summation of the sprung – unsprung mass velocities. That being the case, why do these very different magnitude traces produce the same IRI value? A close examination of Equation (5) reveals the answer. The integral in Equation (5) is actually solved using a summation with the number of samples (n) times the sample increment (dx) replacing the length:

$$IRI = \frac{1}{L} \int_0^{L/V} |\dot{z}_s - \dot{z}_u| dt = \frac{1}{n dx} \sum_{i=1}^n |\dot{z}_{si} - \dot{z}_{ui}| dt \quad (8)$$

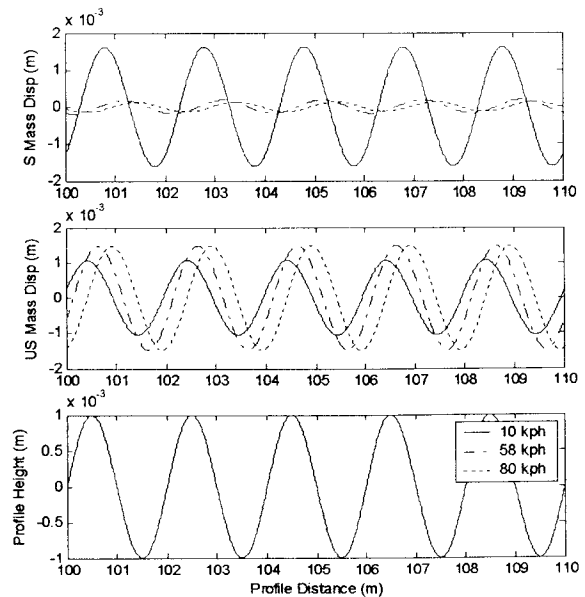


Figure 14 – Sprung and Unsprung Mass Displacement and Profile Height as a Function of Distance for a 0.5 cycle/m Sinusoidal Road Profile

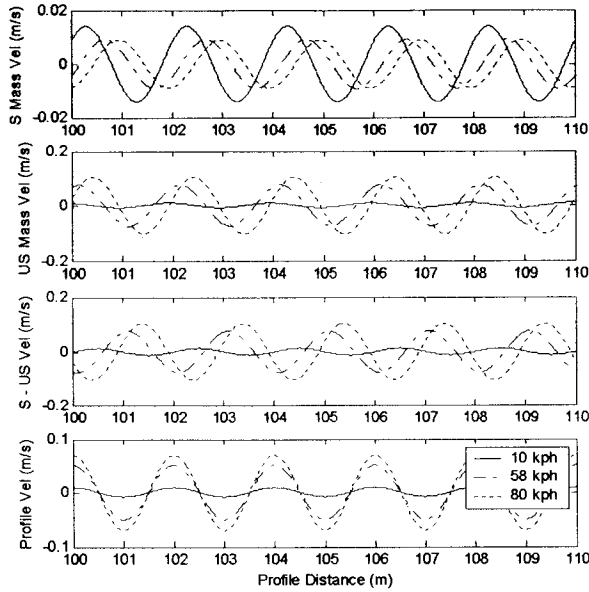


Figure 15 – Sprung, Unsprung, and Sprung - Unsprung Mass Velocities and Profile Velocity as a Function of Distance for a 0.5 cycle/m Sinusoidal Road Profile

Since dx and dt are constants and velocity $V = dx/dt$:

$$IRI = \frac{1}{nV} \sum_{i=1}^n |\dot{z}_{si} - \dot{z}_{ui}| \quad (9)$$

Equation (9) shows that the IRI is inversely proportional to the velocity. This explains how the very different sprung – unsprung mass velocities in Figure 15 for the 10, 58, and 80 km/h speeds can produce the same IRI value.

So even though approximately the same IRI values were produced at 10, 58, and 80 km/h, this does not imply the road harshness at these speeds is the same. Further demonstration of this is given in Figure 16. The spring, damper, suspension (spring + damper), and tire forces are plotted in this figure. Even though the spring force magnitude is approximately the same for all three speeds, the other forces increase with increasing speed.

These results suggest that the IRI formulation will not be appropriate for rating terrain roughness or harshness at multiple speeds. These results have no impact on current road roughness ratings because they are currently carried out at a single speed.

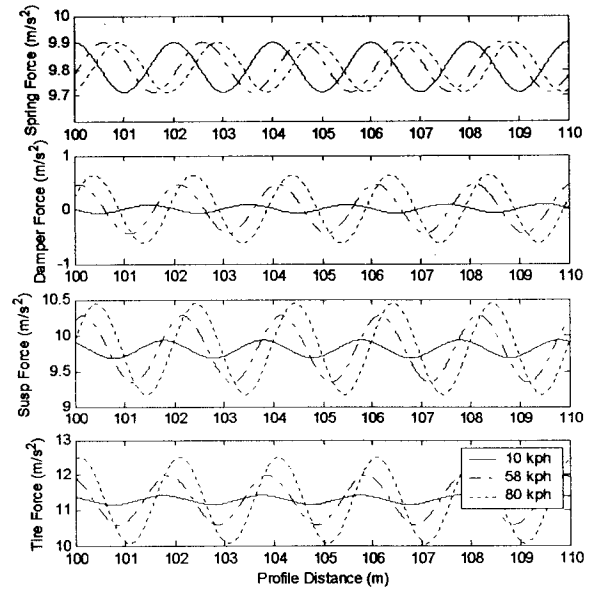


Figure 16 – Spring, Damper, Suspension, and Tire Force as a Function of Distance for a 0.5 cycle/m Sinusoidal Road Profile

SPEED ROUGHNESS INDEX (SRI)

One option for overcoming the deficiency related to rating terrains at various speeds is to take the division by speed out of the IRI calculation. The units for this new metric would be m/hr. This new metric is called the Speed Roughness Index (SRI). Doing this for the IRI values discussed above yields the contour plot shown in Figure 17, which shows SRI as a function of speed and wave number. A surface plot of the same data is given in Figure 18. These plots seem to have more physical meaning. Across speed, the SRI values are highest in the band pass filter frequency range for the given speed. The highest values occur near the second peak of the band pass filter. The SRI values also decrease with decreasing speed (or increase with increasing speed), which again is intuitive given the velocity and force traces in the previous figures. The decrease in SRI values as speed decreases and wave number increases (upper right sweeping down and then towards lower left in Figure 17) is due to the moving average tire model.

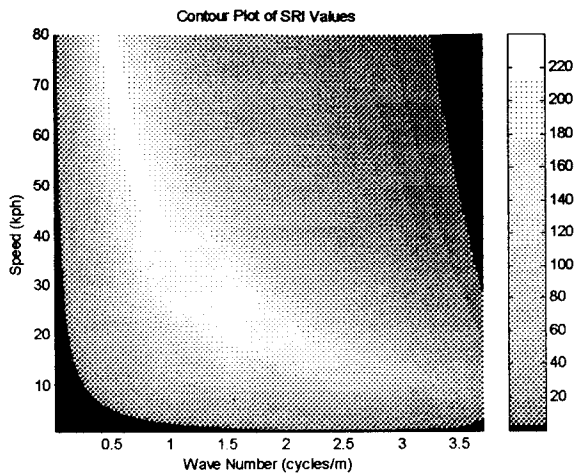


Figure 17 – Contour Plot of SRI Values as a Function of Wave Number and Speed

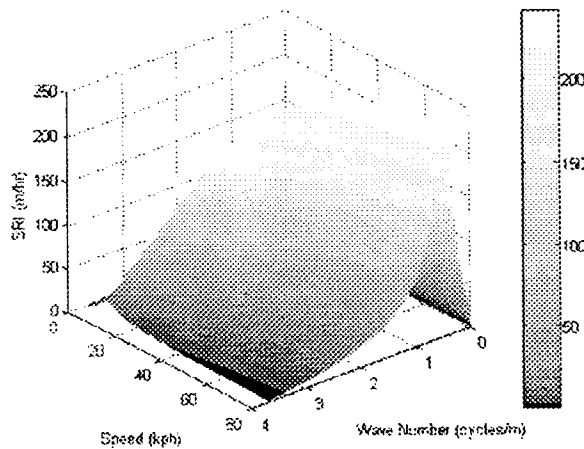


Figure 18 – Surface Plot of SRI Values as a Function of Wave Number and Speed

REPETITIONS TO FAILURE

As noted above, an important element of this program is the development of means to include fatigue failure factors in the terrain rating procedure. In the work to date, basic established fatigue analysis methods have been applied in conjunction with the quarter car model to obtain an initial understanding of trends. This involved the use of suspension force as opposed to the suspension velocity used in the IRI. The suspension force was applied to a hypothetical structural element with a specified cross-sectional area to obtain a representative stress time history. Once the stress time series was known, it was sent to a “rainflow” counting algorithm [8]. The results of the rainflow counting were then used to determine the repetitions required to reach failure for the given terrain.

Fatigue life estimation is fundamentally based on the Wöhler Stress vs. Number of Cycles to Failure (S-N)

curve. An example of this type of curve is given in Figure 19. The S-N curve relates fatigue life (the number of cycles to failure, N_f) to stress amplitude expressed as “alternating stress” (σ_a).

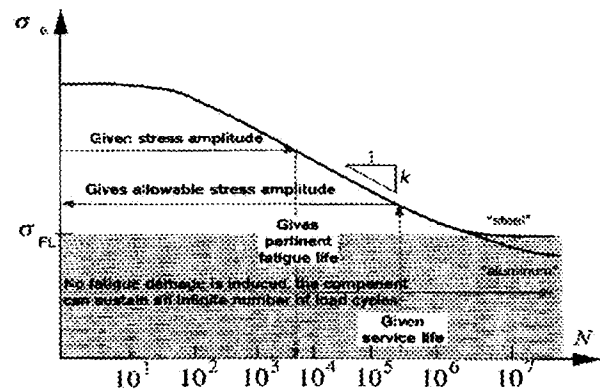


Figure 19 - Wöhler S-N Curve [7]

The stress time series anticipated in components of military vehicles operating in off-road conditions will be relatively complex. Figure 20 shows a hypothetical example of what might be expected from terrain-induced stress. For fatigue analysis of the general loading case depicted in Figure 20, application of the “rainflow” cycle counting algorithm, introduced by Endo in 1968 [8], is now common practice.

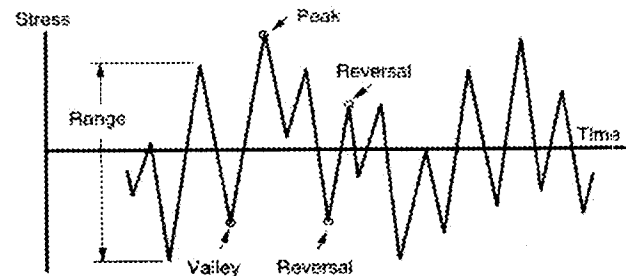


Figure 20 – Arbitrary Loading Time History [9]

The rainflow counting process is quite laborious for almost any practical stress time history, but the algorithm can and has been implemented in software. A suitable software package, called WAFO (Wave Analysis for Fatigue and Oceanography), is available in the public domain (<http://www.maths.lth.se/matstat/wafo>). WAFO was developed by the Mathematical Statistics Center for Mathematical Science at Lund University in Sweden and provides comprehensive tools as a MATLAB toolbox for wave and fatigue analyses and simulations. WAFO contains numerous routines for evaluating fatigue measured loads, as well as making theoretical calculations of distributions that are important for fatigue evaluation.

The number of cycles to failure of any well designed military vehicle component will in all likelihood be very much larger than those contained in any test or simulation time series analyzed. Thus, it is quite

impractical to work with a time series representing the complete fatigue life of a component. Instead it is feasible to obtain or generate a much shorter stress time series, which is still long enough to capture the statistics of a given terrain profile. This practical profile can then be applied repeatedly in the fatigue analysis using the Palmgren-Miner equation (Ref. 9).

$$B_f \left[\sum_{i=1}^n \left(\frac{\eta_i}{N_{f_i}} \right) \right]_{\sigma_i = \text{const}} = 1 \quad (10)$$

one repetition

The number of repetitions of the profile, B_f , instead of the percentage of entire service life, provides the measure of the expected fatigue life.

The repetitions to failure for the sinusoidal terrains have been determined using the suspension force time histories for each of the individual runs at each speed and wave number combination given above.

The sprung mass is not a known quantity in the IRI calculation. The total sprung mass for the vehicle was assumed to be 1460 kg (100 slugs) and therefore the sprung mass for the quarter car was 365 kg (25 slugs). The arbitrary stress element was chosen to be a circular rod with a radius of 0.0025 meters. The definition of parameters such as this is but one of many fatigue issues to be further investigated for this work.

At high frequency and high speed, the initial IRI quarter car response was affected by some high frequency component of the input, before settling into a constant-amplitude oscillatory motion. To keep the initial transients from entering the determination of the repetitions to failure, only cycles 150 to 450 (out of 500) were used in the analysis. The repetitions to failure given below are repetitions of the 300 cycles; in other words it is the number of times required to repeat the 300 cycles for failure to occur. To get a number of repetitions to failure for an individual cycle, the numbers given below would need to be multiplied by 300.

It should be noted that the repetition to failure values presented below are not normalized for profile length. They are based on having the same number of oscillations regardless of the wave number.

It was found that the repetitions to failure were many orders of magnitude different for various speed/wave number combinations. This being the case, the log (base 10) of the repetitions to failure values are presented in the figures below.

A contour plot of the repetitions to failure as a function of speed and wave number is given in Figure 21. To provide more contrast in the region of interest, this plot was limited to 30. The values in the lower right hand corner of the plot reach over 60. This plot looks very

similar to the SRI contour plot given in Figure 17. The main difference is that the dark and light areas are reversed. This is because a harsher road input results in a lower number of repetitions to failure, while the opposite is true for SRI (a harsher road input results in a higher SRI). A surface plot of the same data is shown in Figure 22. This plot again is similar in shape to that for the SRI plot except it is inverted. The increase in the repetitions to failure as the speed decreases and wave number increases is due to the moving average tire model.

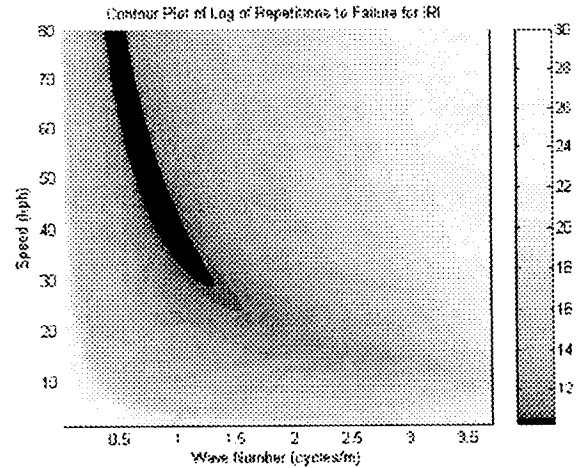


Figure 21 – Contour Plot of Repetition to Failure Values as a Function of Wave Number and Speed

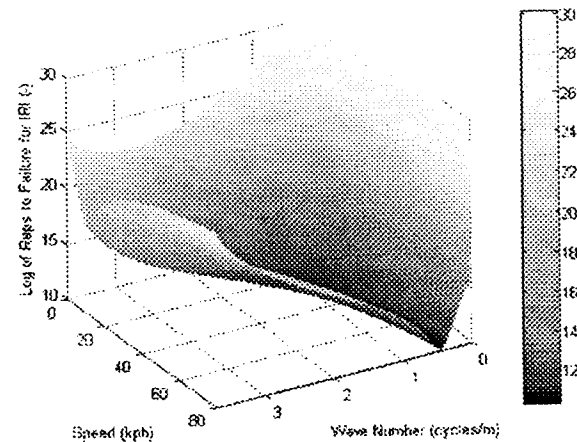


Figure 22 – Surface Plot of Repetition to Failure Values as a Function of Wave Number and Speed

CONCLUSION

Properly characterizing terrain roughness is an important issue for the U.S. Army. An approach to solving this problem is to examine the response(s) of a relatively simple vehicle model driven over the terrain/test course and developing a metric to characterize the roughness of the terrain. One example of this type of index is the IRI.

The results presented in this paper suggest that the IRI formulation will not be appropriate for rating terrain roughness or harshness at multiple speeds. These results have no impact on current road roughness ratings because they are currently carried out at a single speed. One option for overcoming this deficiency for rating terrains at various speeds is to take the division by speed out of the IRI calculation (multiply IRI by Speed = SRI). Another option is to use suspension force as a metric in combination with rainflow counting stress algorithms to determine a Repetition to Failure for the given terrain.

REFERENCES

1. Gorsich, D. J., et. al. "Terrain Roughness Standards for Mobility and Ultra Reliability Prediction," SAE 2003-01-0218.
2. Gillespie, T., "Analysis of APG Test Program for the M1000 Heavy Equipment Transporter," University of Michigan Engineering Consultation, 1994.
3. Sayers, M. W., "On the Calculation of International Roughness Index from Longitudinal Road Profile," TRR 1501 – Pavement-Vehicle Interaction and Traffic Monitoring, 1995.
4. Karamihas, S. M., Gillespie, T. D., Perera, R. W., Kohn, S. D., "Guidelines for Longitudinal Pavement Profile Measurement", National Cooperative Highway Research Program Report 434, Transportation Research Board, 1999.
5. Guo, K., "Tire Roller Contact Model for Simulation of Vehicle Vibration Input," SAE paper No. 932008.

6. Guo, K., "A Model of Tire Enveloping Properties and its Application on Modeling of Automobile Vibration Systems," SAE paper No. 980253.
7. Ekberg, A. "Lecture Note on Fatigue and Crash Course," Department of Solid Mechanics, Chalmers University of Technology, Sweden, www.solid.chalmers.se/ane/teaching/fatfract/
8. Matsuishi, M. and Endo, T. "Fatigue of Metals Subjected to Varying Stress," paper presented to Japan Soc. Mech. Engrs., Jukvoka, Japan, 1968.
9. Dowling, N. E., "Mechanical Behavior of Materials-2nd Edition," Prentice Hall, 1998.

CONTACT

J. Gavin Howe

Systems Technology, Inc.
13766 S. Hawthorne Blvd
Hawthorne, CA 90250-7083
url: <http://www.systemstech.com>
e-mail: gavin@systemstech.com

DEFINITIONS, ACRONYMS, ABBREVIATIONS

IRI: International Roughness Index

SRI: Speed Roughness Index = IRI x Speed